Proceedings of ICFDP9:
Ninth International Congress of Fluid Dynamics & Propulsion
December 18-21, 2008, Alexandria, Egypt

ICFDP9-EG-250

C.F.D ANALYSIS OF BOUNDARY LAYER GROWTH WITHIN A TRANSONIC WIND TUNNEL TEST SECTION

Mohammad Javad Izadi
Bu-Ali Sina University
Mj_izadi@hotmail.com

Abedin Shokri
Bu-Ali Sina University
Ab_shokri@yahoo.com

ABSTRACT

With due consideration to high expenses in obtaining experimental results of aerodynamic coefficients, getting precise results from some numerical codes is very important to all engineers. In this work, the boundary layer growth, in the test chamber of a transonic wind tunnel is studied. In this study the dimensions of the test chamber are modeled as $0.3048*0.3048*0.3048\ m^3$ ($1*1*1\ ft^3$), and the test section Mach number is taken to be between 0.7 and 1.2.

The computation is done using Spalart-Allamaras method. Considering the wall boundary layer growth of the test section obtained from the numerical code, the best location placing an object inside the tunnel is to locate it outside the boundary layer and that is to place the model far from the walls toward the center of the tunnel of the test section. The maximum thickness of the boundary layer is found to be about 0.0058 m at the end of the wind tunnel test section.

KEYWORDS:

Boundary layer, Wind tunnel, transonic flow.

INTRODUCTION

Wind tunnels have long been used as tools for aerodynamic research, development, and testing, so their use is relatively well understood. However, it is possible that the undefined obtained data's from the wind tunnel might be more excessive because of the large action and reaction between the fluid and the geometric constrains, though using the wind tunnels are acceptable.

Nowadays many of aerospace industries and laboratories are equipped with subsonic up to hypersonic wind tunnels, such as transonic tunnels. In this research, the test chamber of a transonic wind tunnel is modeled and since the flow is turbulent and for faster solution, the Spalart–allmaras model has been selected among the existing models and the problem is analyzed.

THE MODEL

The Spalart–allmaras models are belong to the family of eddy viscosity models. This family of models is based on the assumption that the Reynolds stress tensor ($\rho\overline{u_i u_j}$) is related to the mean strain rate through an apparent turbulent viscosity, called eddy viscosity v_T.

$$-\overline{u_i u_j} = v_\tau \left(\frac{\partial \overline{u_i}}{\partial y^j} + \frac{\partial \overline{u_i}}{\partial y^i}\right) \tag{1}$$

In The Spalart–allmaras models, the eddy viscosity is computed through a partial differential equation. In particular, the eddy viscosity v_T is computed by an intermediate variable $\tilde{v}$ through the relation

$$v_\tau = \tilde{v} f_{v1}(x) \tag{2}$$

Where, X is a ratio as bellow

$$X = \frac{\tilde{v}}{v} \tag{3}$$

And f_{v1} is a damping function. The intermediate variable $\tilde{v}$ is computed by solving a differential equation that can be written in a compact form as:

$$\frac{D\tilde{v}}{Dt} = b_{prod}(S, \tilde{v}, d) - b_{dest}(\tilde{v}, d) + b_{trip}(d_T) + \frac{1}{\sigma}[\nabla.((v + \tilde{v})\nabla\tilde{v}) + c_{b2}(\nabla\tilde{v})^2] \tag{4}$$

Where the symbols b_{prod} and b_{dest} indicate respectively the production term and the destruction term, and finally b_{trip} denotes a special source term which allows the laminar-

turbulent transition in a fixed point. It should be pointed out that, although the transition onset point has to be user-specified, the flow development in the transition region is built into the model through this trip source term. The quantities enclosed between the brackets, show the main depending variables of these source terms.

In particular, $_s$ denotes the vorticity magnitude, $_d$ is the wall distance and $_{d_T}$ is the distance from the transition point. The last term in the right hand side is a diffusion term in which $_\sigma$ and $_{c_{b2}}$ denote respectively the turbulent Prandtl number and a calibration constant respectively.

GEOMETRICAL MODEL AND SOLUTION NETWORK

A chamber of 0.3048*0.3048*0.3048 m^3 dimension is prepared. For simplicity and because of the symmetry, the tunnel is divided into four equal areas (Figure 1). The quarter inlet area of the test section studied here is 0.1524m by 0.1524m (width and height) with 0.3048m. in length as presented in Figure 2.

The plates I and IV from the block modeled here have symmetrical condition with respect to the top and left blocks within the test section and the coordinate direction is the same direction which is indicated in Figure 2, and the origin of the coordinate system is assumed at the entrance of the tunnel.

As the meshes approach near the wall, they become smaller, thus by moving in the direction of positive z, the size of the nodes become smaller and by moving downward, that is from positive y to zero, the number of nodes increases. For the x-y plate, the meshing must be selected in a manner that at the input region, the dimensions of meshes becomes smaller because of the boundary layer formation (Figure 3, 4). In order to obtain a better accuracy of results, different grids are considered at the beginning and at last when the results converged to a similar number, the final number of grids is selected.

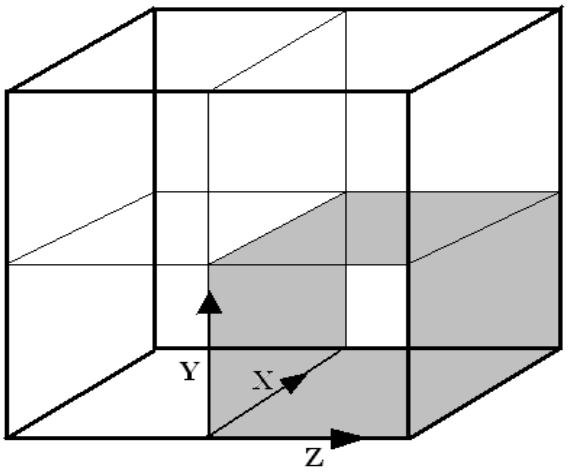

Figure 1- The test section of the transonic wind tunnell

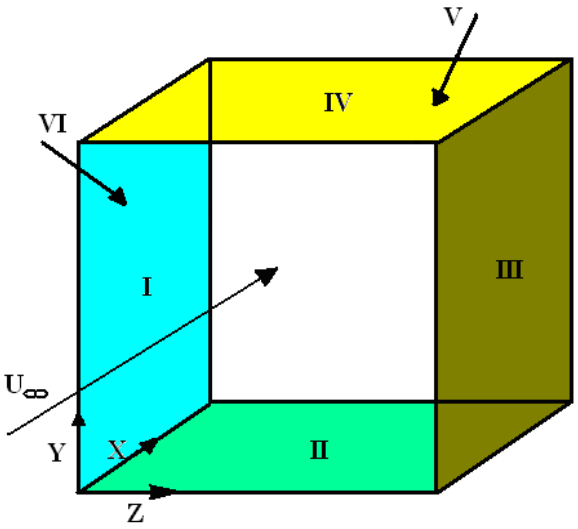

Figure 2- Quarter section of the wind tunnel test section

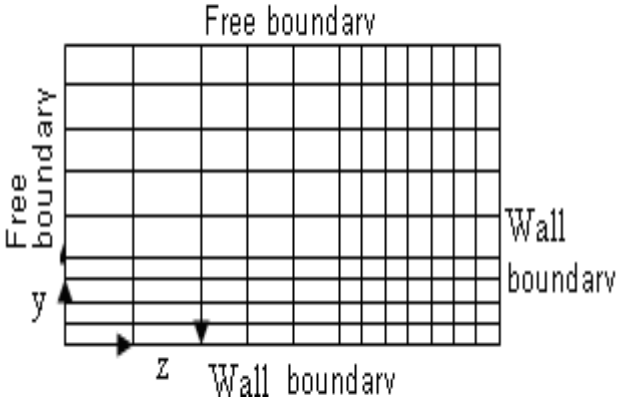

Figure 3- Mesh networking in y-z plate

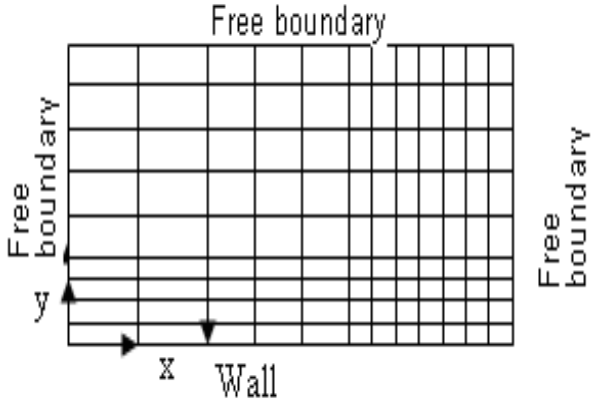

Figure 4- Mesh networking in y-x plate

BOUNDARY CONDITION

For plates II and III or the walls, the no-slip condition is enforced. The plates I and IV or the planes of symmetry have the free boundary condition, and the inlet plate or plate VI has the inlet velocity (defined by user) and the plate V has the outlet pressure.

DISSCUSSION

On the surface of the wall where the no-slip condition is enforced, at a fixed point on the z axis, as the free stream velocity increases, the thickness of the boundary layer decreases, and that is because, the friction force overcome the momentum force and because of the existence of the sub layer in the turbulent region which causes a decrease in the boundary layer. But, as the free stream velocity become larger than the speed of sound (Supersonic), at the entrance of the wind tunnel section, the free stream become move turbulent and this will effect the downstream flow and causes the velocity near the surface to decrease and this causes the boundary layer thickness to increase suddenly for Mach number greater then one (Figures 5 and Figure 6).

Near the wall, the thickness of the boundary layer in the subsonic flow, increased (Figures 7, 8 and 9) and in the supersonic flow, at the end of the wind tunnel section, the boundary layer thickness decreased (Figures 10 to 14). In the subsonic flow and near the wall, the thickness of the boundary layer for the Mach numbers of 0.7, 0.8, and 0.9, equally increased throughout the wind tunnel section (Figures 15, 16, 17). In the supersonic flow from the beginning to near eighty percent length of the tunnel, (0.8 length of the test section), the boundary layer thickness increases and after that, suddenly decreases (Figures 18,19, 20).

CONCLUSION

From the numerical results of this study, the best area of placing an model within the test section of any wind tunnel, is an area outside the boundary layer thickness, and in a transonic wind tunnel test t section, the best area is about 98.1 percent of the physical area.

The maximum boundary layer thickness at the end of the test section is found to be about 0.0058m.

In the subsonic region, when the velocity of the flow increased up to Mach one, the thickness of the boundary layer decreased, and when the flow velocity increased to Mach 1.1, the thickness of the boundary layer increased and for Mach numbers higher than 1.1, the Boundary layer thickness (B.L. thickness) decreased again similar to that of subsonic region.

Near the wall at the end of the tunnel, when flow is considered to be subsonic, the thickness of the boundary layer decreased. At Z=0.4995 for Mach=1, the B.L. thickness is calculated to be 0.0036m and for Mach=1.1, the thickness of the Boundary layer was 0.0015m, and for Mach=1.2, the B.L. thickness is calculated to be about 0.003m.

NOMENCLATURE

b_{prod}	production term
b_{dest}	destruction term
b_{trip}	special source term
c_{b2}	calibration constant
d	wall distance
d_T	distance from the transition point
f_{v1}	damping function
M	Mach number
S	vorticity magnitude
u	Velocity
U_∞	Free stream velocity
v_T	eddy viscosity
$\tilde{v}$	intermediate variable
σ	turbulent Prandtl number
ρ	Air density

REFERENCES

[1]. P. Spalart and S. Allmaras. A one-equation turbulence model for aerodynamic flows. Technical Report AIAA-92-0439, La Recherché Aerospatiale. (1):5-21.1994.

[2]. J. L. Everhart and P.J. Bobbit. Experimental Studies of Transonic Flow Field Near a Longitudinally Slotted Wind Tunnel Wall. La Recherché center NASA TP 3392.1994.

[3]. R. Paciorri and W. Dieudonnéy and G. Degrez z J. and M. Charbonnierx and H. Deconinck.validation of the Spalart–allmaras turbulence models for application hypersonic flow. von Karman Institute for Fluid Dynamics Sint-Genesius-Rode, Belgium.1997.

[4]. P. Spalart and S. Allmaras. A one-quation turbulence model for aerodynamic flows. Technical Report AIAA-92-0439, American Institute of Aeronautics and Astronautics, 1992.

[5]. H. Schlichting. Boundary layer theory. McGraw-Hill, New-York, 1968. Chap. 23.

[6]. s. m. Gorlin and I. I. Slezinger. Wind tunnel and their instrumentation. Izdatel'stvo "nauka". Moska.1964

[7]. T. L. Campioli and J.Schetz and R. E. Neel. Assessment of incompressible formulations for numerical solutions of unsteady turbulent flows over bluff bodies. Technical Report AIAA-1359, American Institute of Aeronautics and Astronautics, 2005.

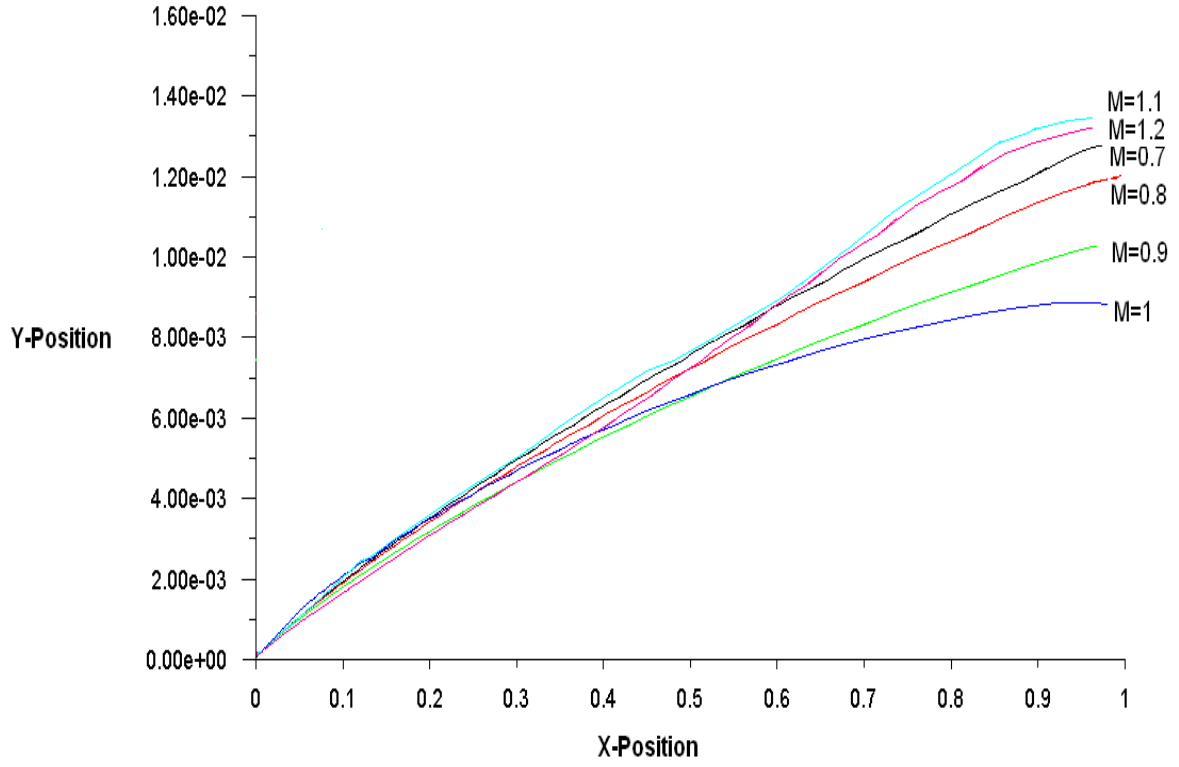

Figure 5-Thicknessof the boundary layer at Z=0.25
(All positions are non-dimensioned base on the length of the test section of the tunnel)

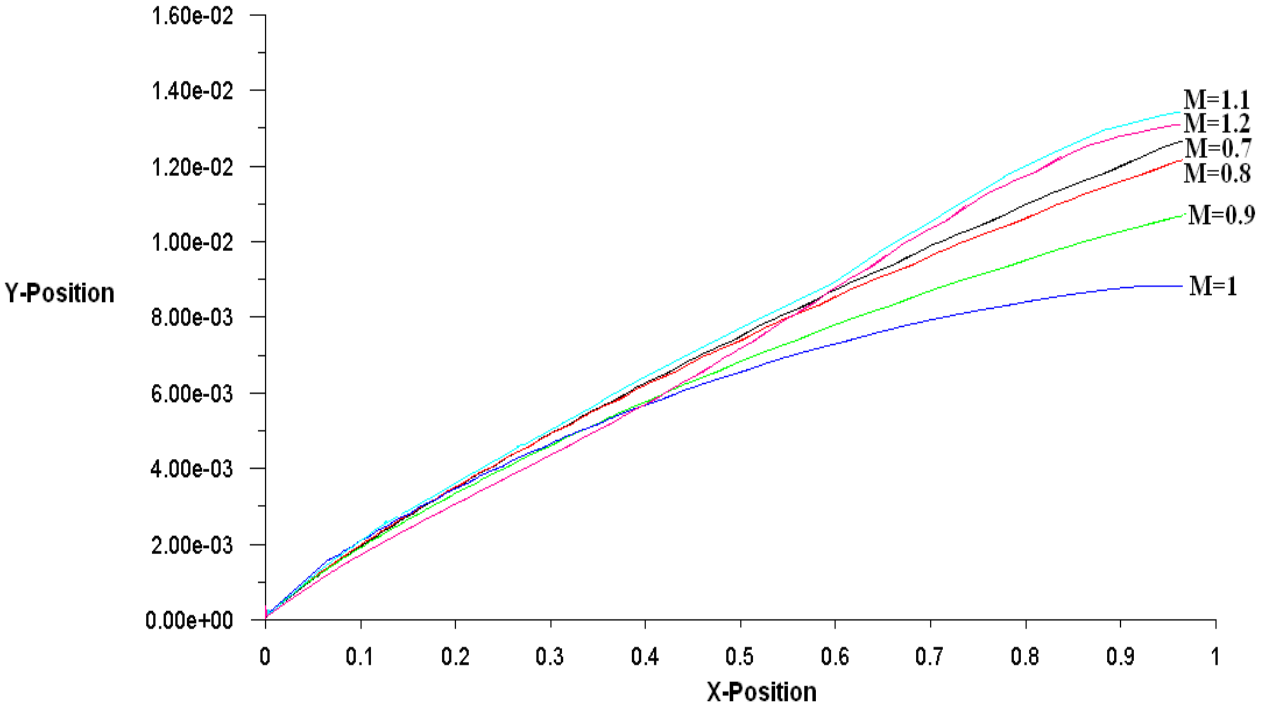

Figure 6-Thickness of the boundary layer at Z=0.4
(All positions are non-dimensioned base on the length of the test section of the tunnel)

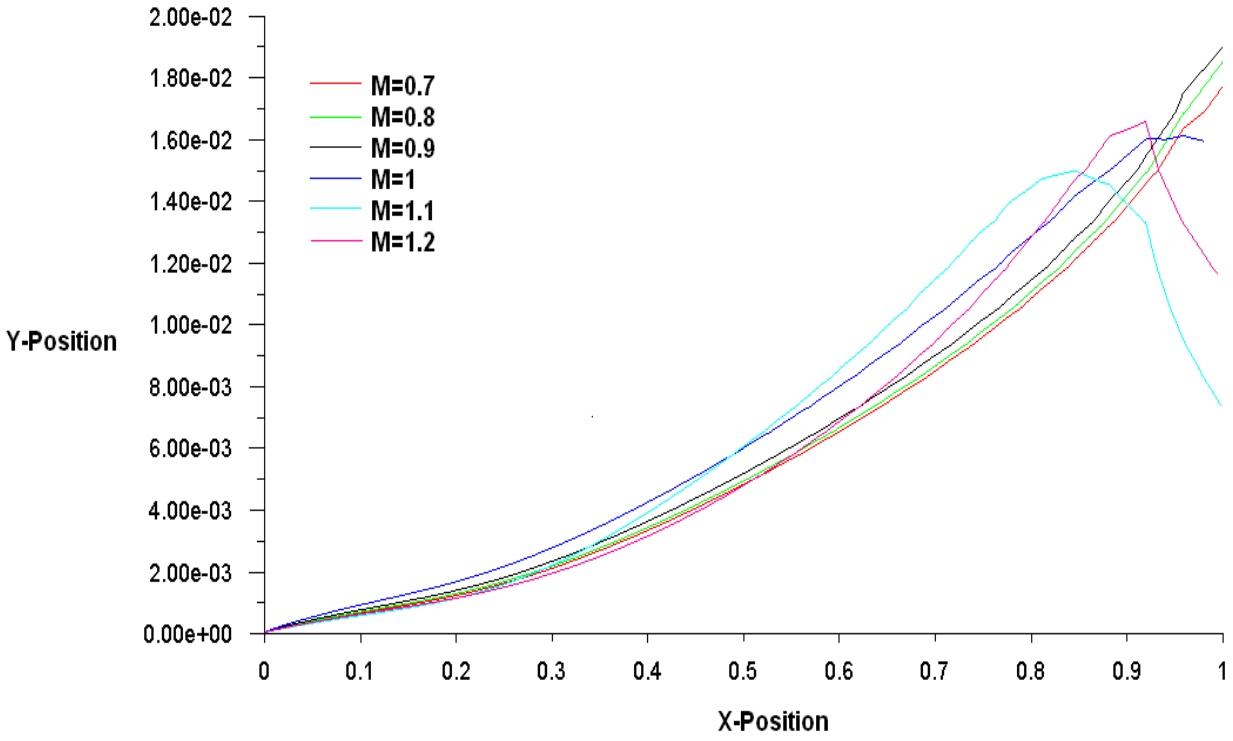

Figure 7-Thickness of the boundary layer at Z=0.4960
(All positions are non-dimensioned base on the length of the test section of the tunnel)

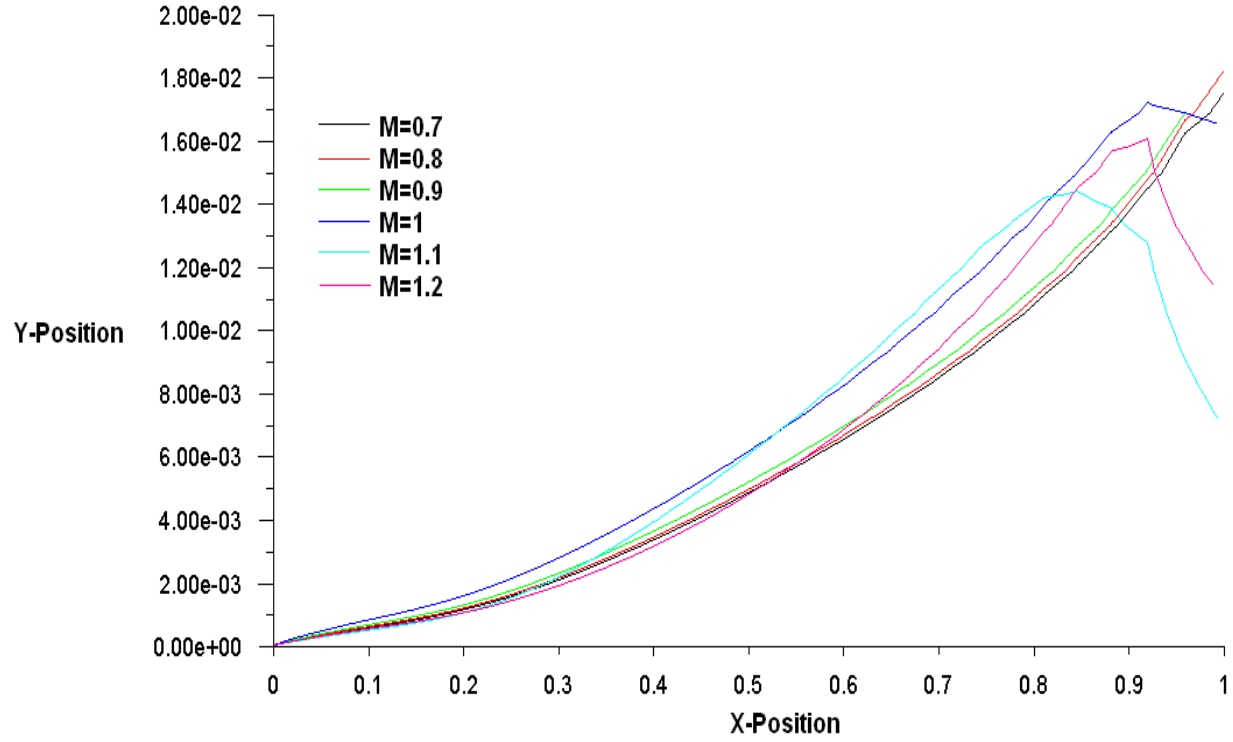

Figure 8-Thickness of the boundary layer at Z=0.4965
(All positions are non-dimensioned base on the length of the test section of the tunnel)

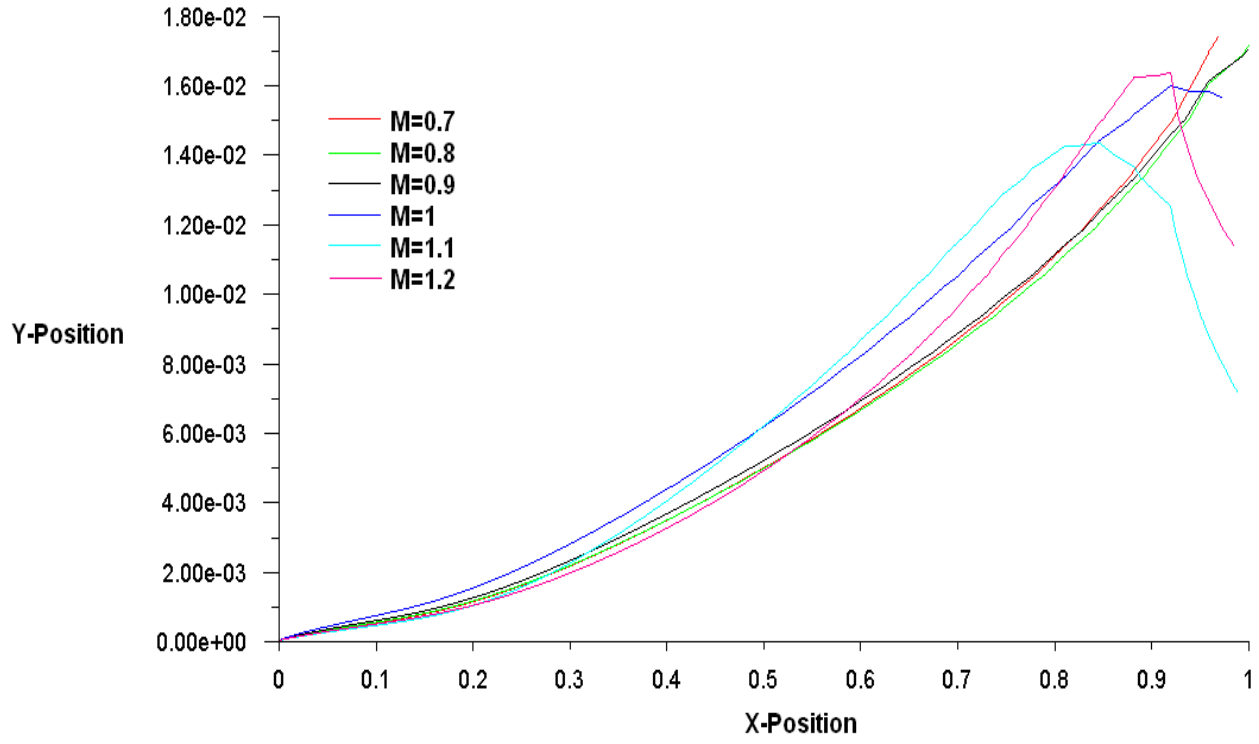

Figure 9-Thickness of the boundary layer at Z=0.4970
(All positions are non-dimensioned base on the length of the test section of the tunnel)

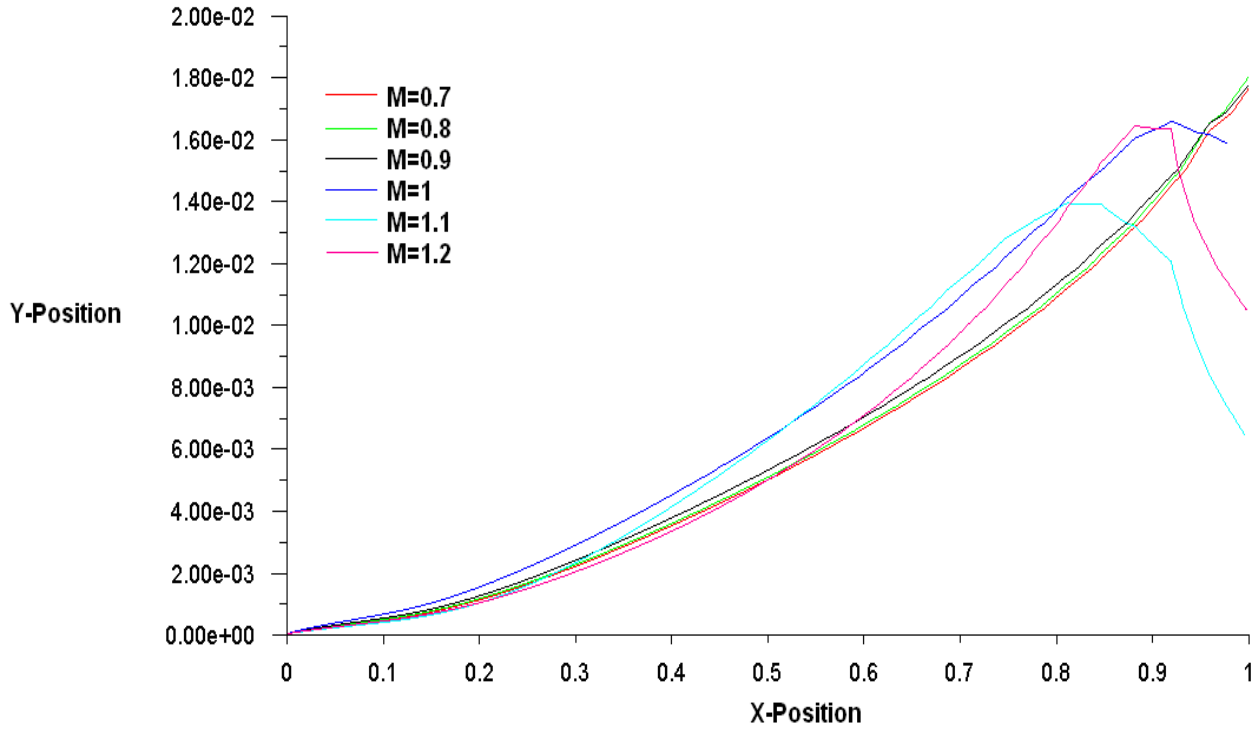

Figure 10-Thickness of the boundary layer at Z=0.4965
(All positions are non-dimensioned base on the length of the test section of the tunnel)

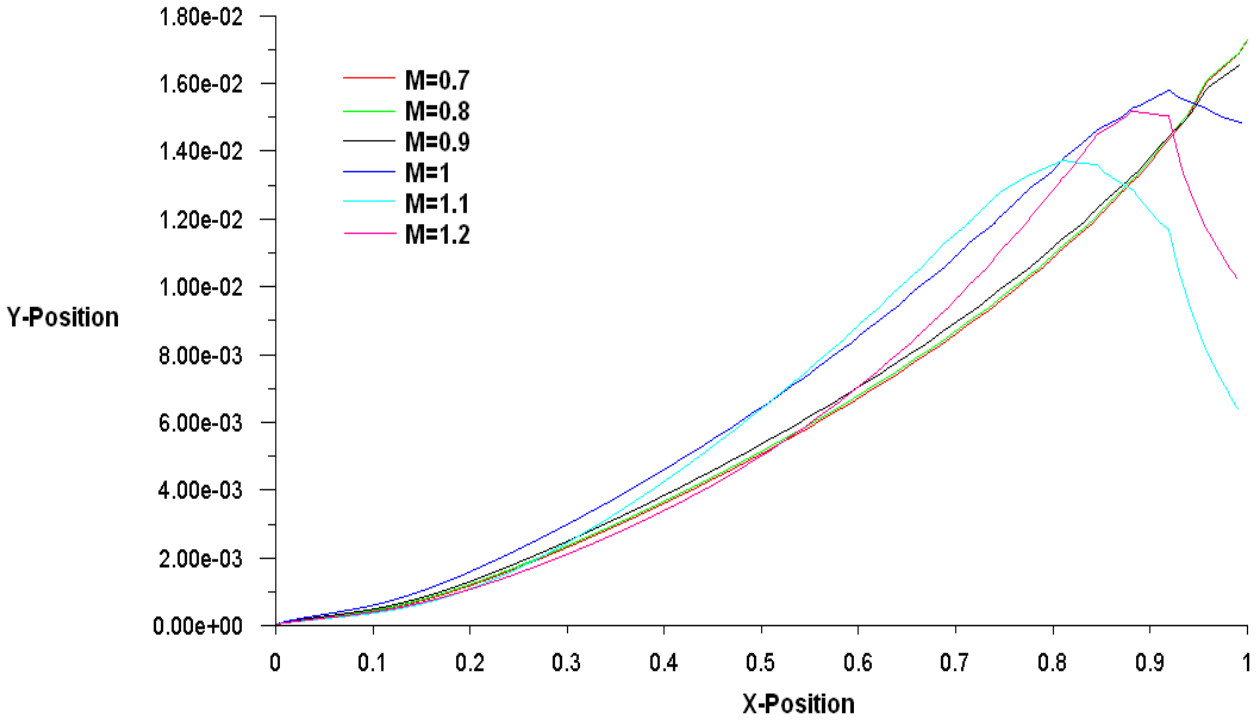

Figure 11-Thickness of the boundary layer at Z=0.4980
(All positions are non-dimensioned base on the length of the test section of the tunnel)

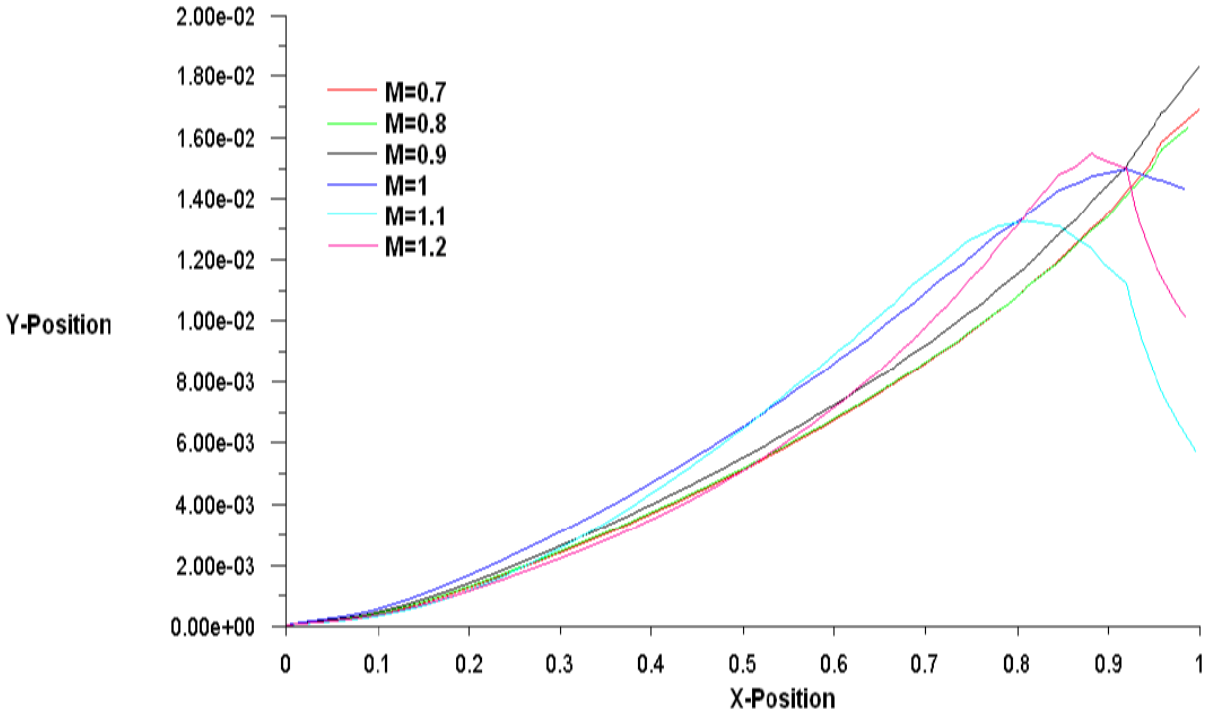

Figure 12-Thickness of the boundary layer at Z=0.4985
(All positions are non-dimensioned base on the length of the test section of the tunnel)

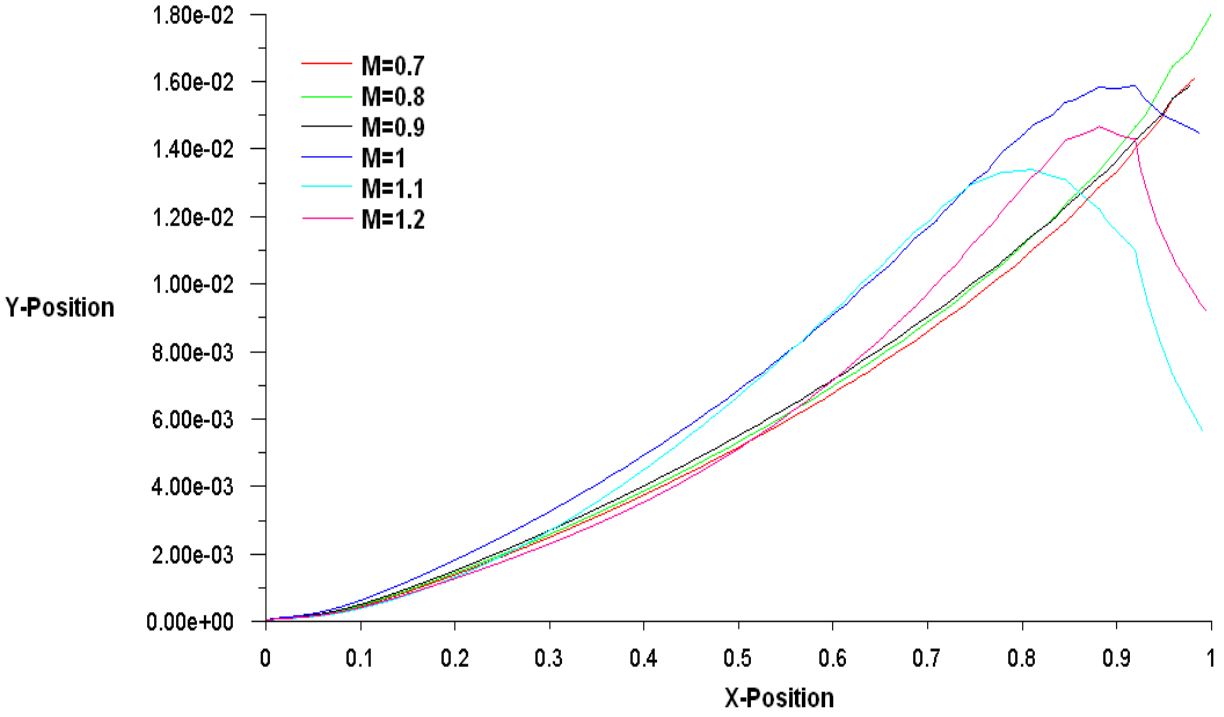

Figure 13-Thickness of the boundary layer at Z=0.4990
(All positions are non-dimensioned base on the length of the test section of the tunnel)

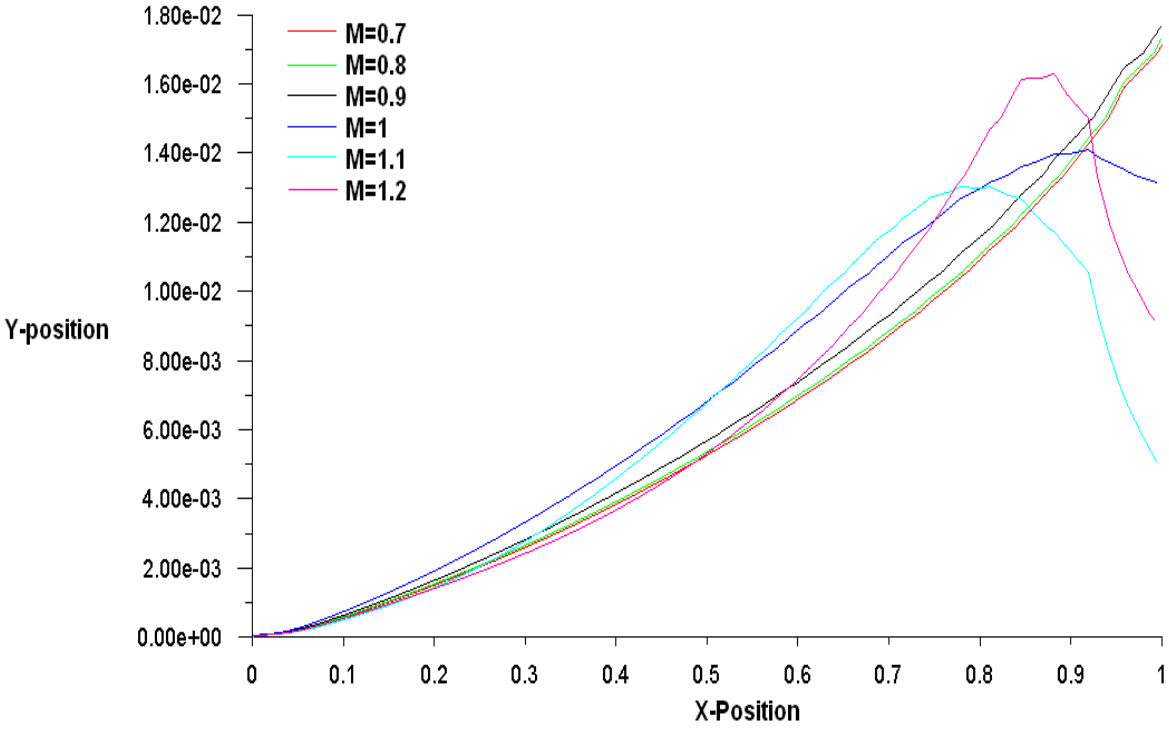

Figure 14-Thickness of the boundary layer at Z=0.4995
(All positions are non-dimensioned base on the length of the test section of the tunnel)

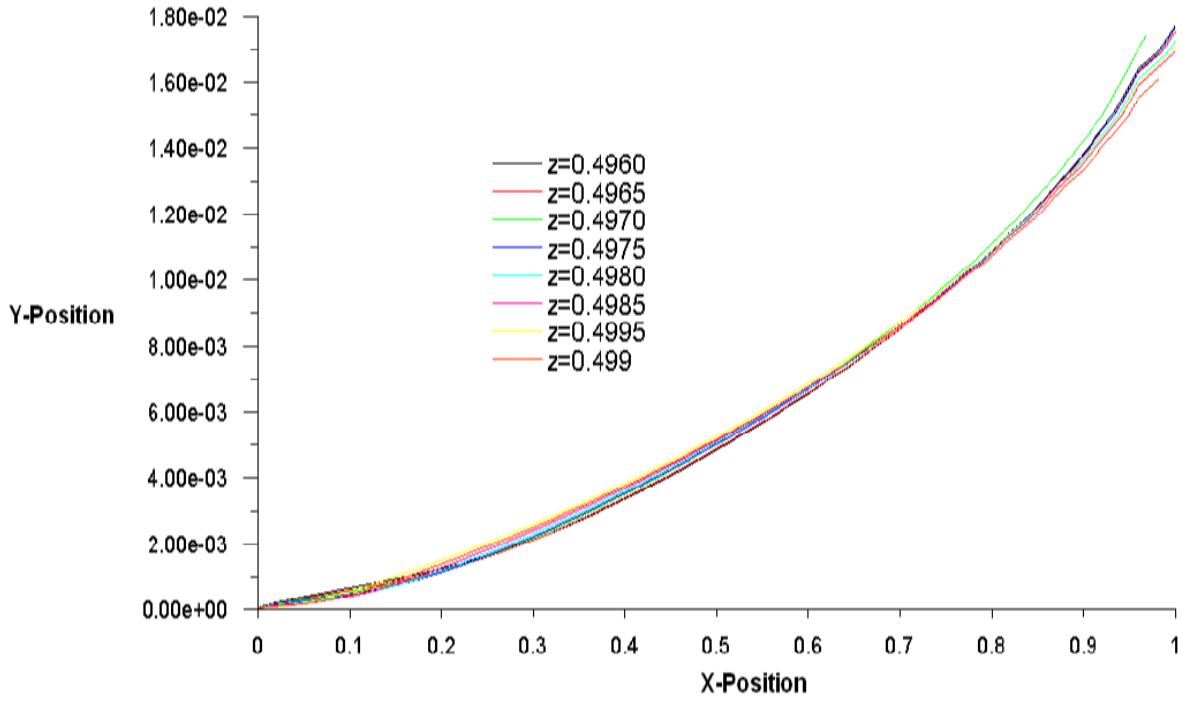

Figure 15-Thickness of the boundary layer near the wall for Mach=0.7
(All positions are non-dimensioned base on the length of the test section of the tunnel)

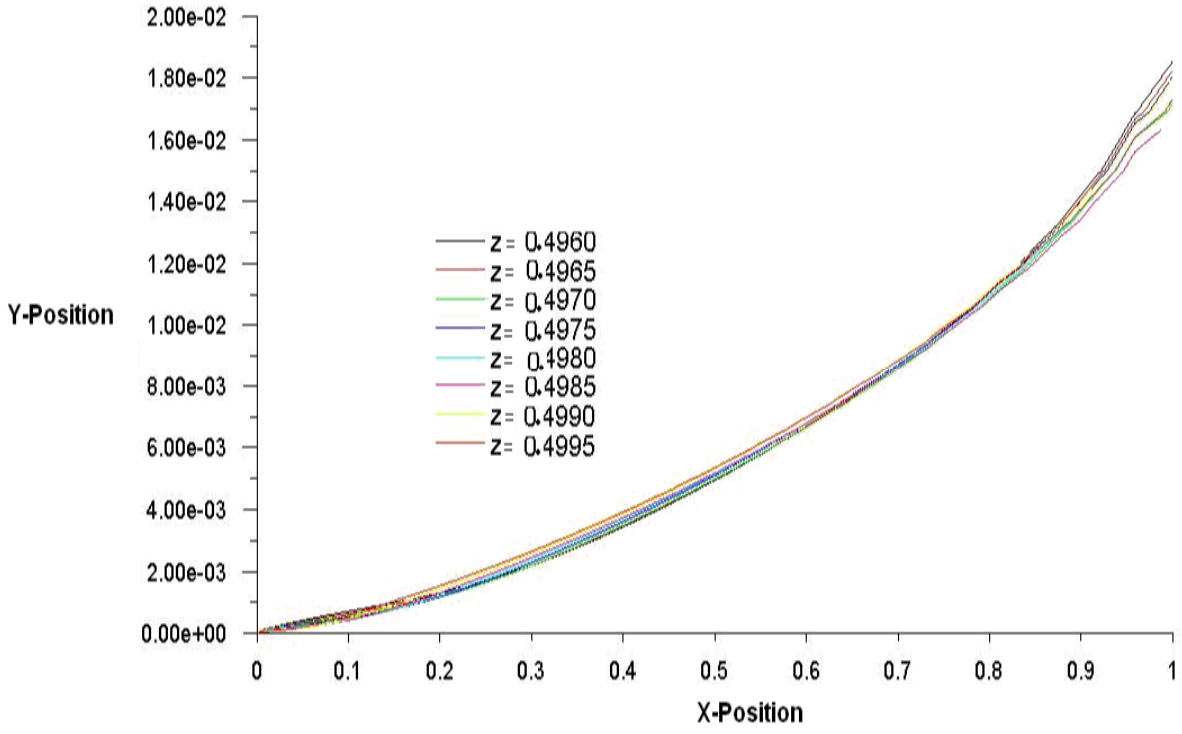

Figure 16-Thickness of the boundary layer near the wall for Mach=0.8
(All positions are non-dimensioned base on the length of the test section of the tunnel)

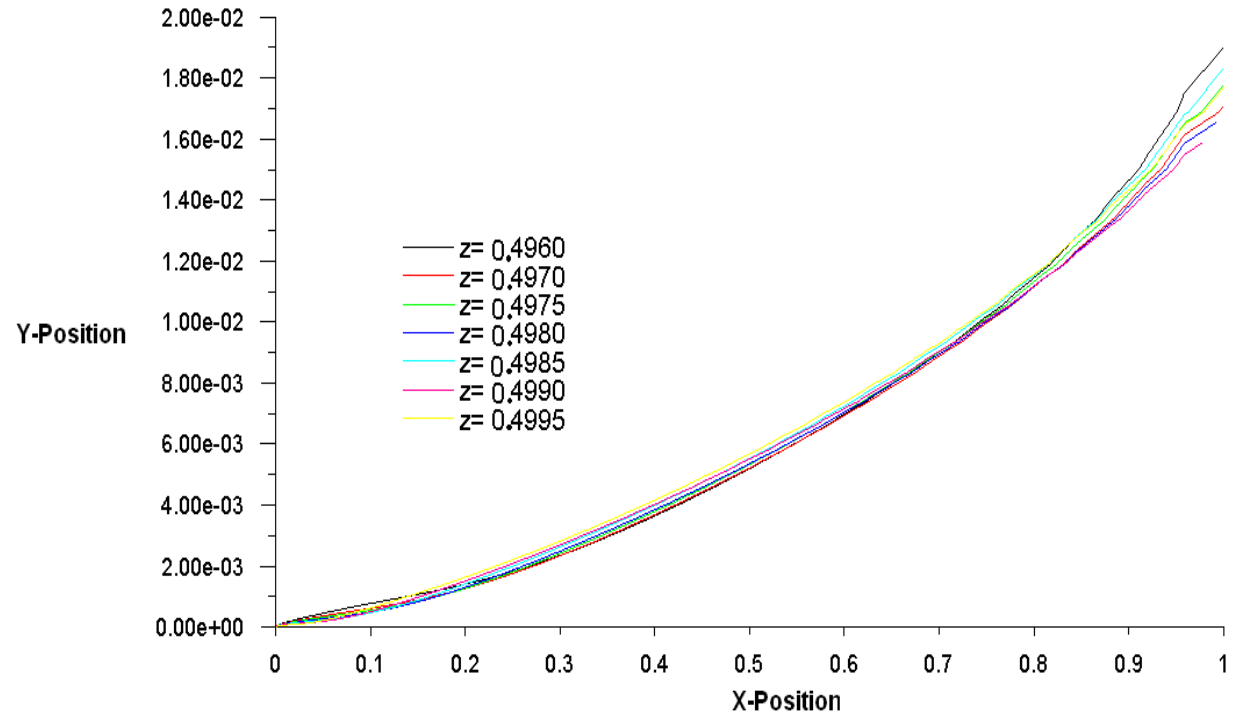

Figure 17-Thickness of the boundary layer near the wall for Mach=0.9
(All positions are non-dimensioned base on the length of the test section of the tunnel)

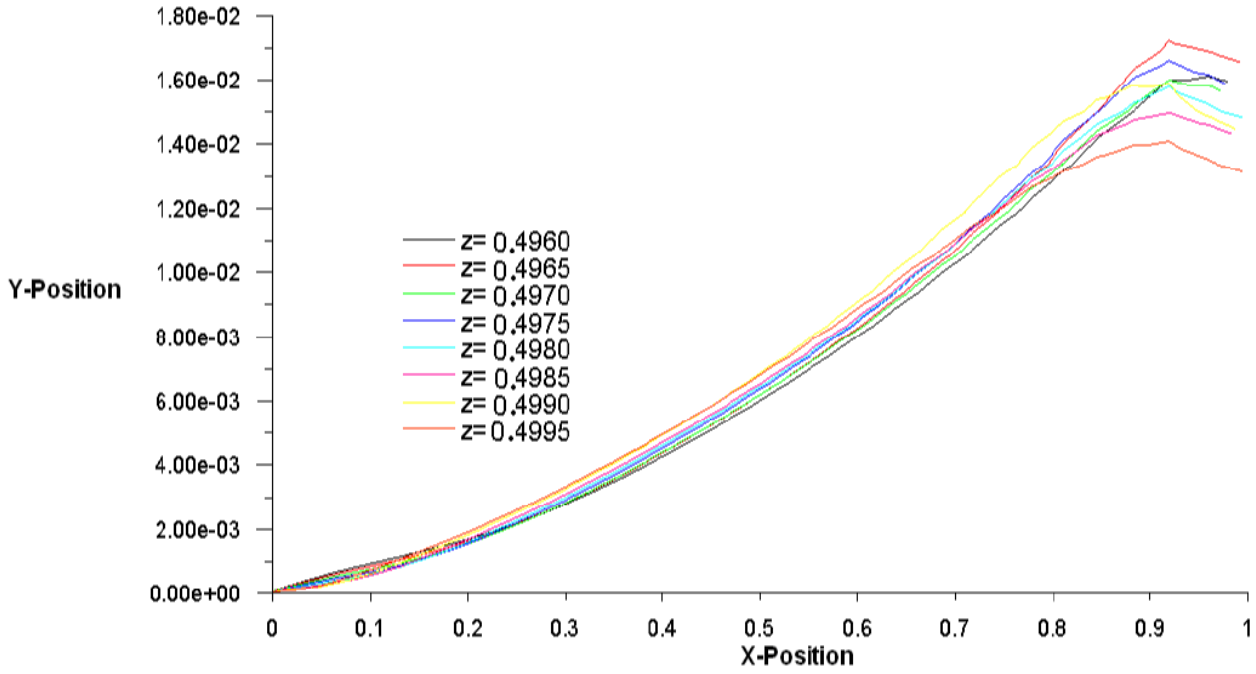

Figure 18-Thickness of the boundary layer near the wall for Mach=1
(All positions are non-dimensioned base on the length of the test section of the tunnel)

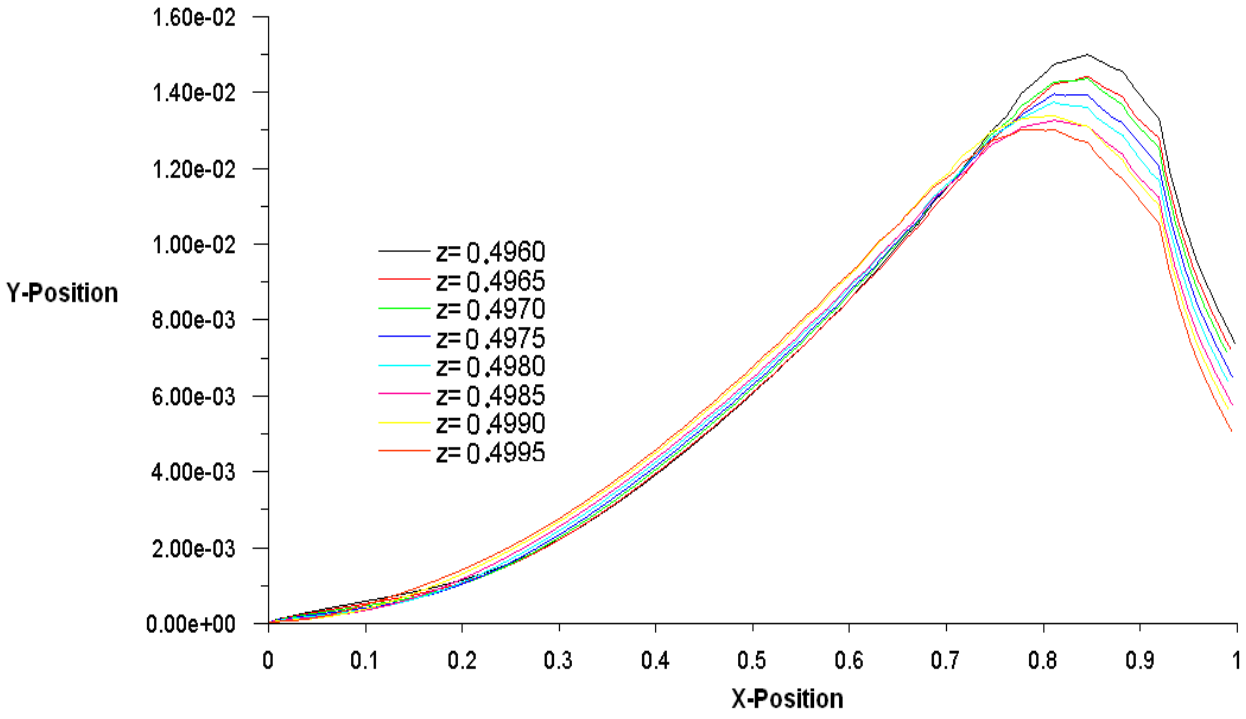

Figure 19-Thickness of the boundary layer near the wall for Mach=1.1
(All positions are non-dimensioned base on the length of the test section of the tunnel)

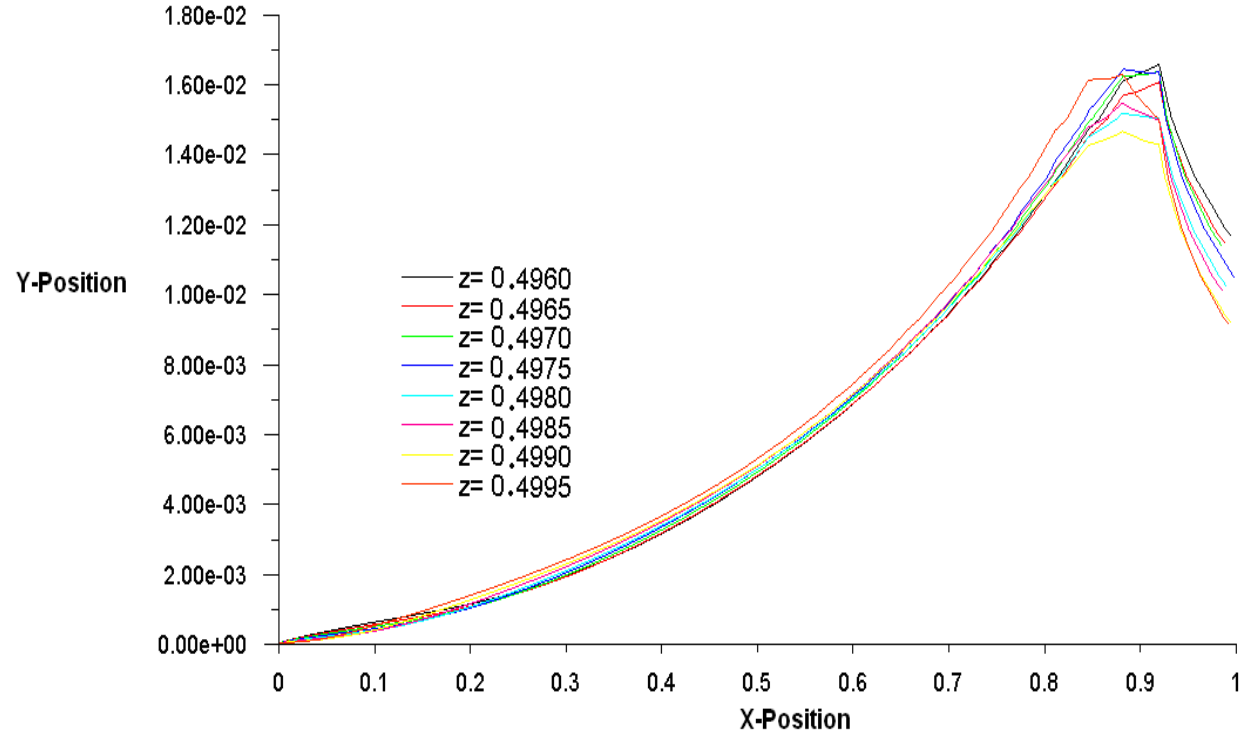

Figure 20-Thickness of the boundary layer near the wall for Mach=1.2
(All positions are non-dimensioned base on the length of the test section of the tunnel)